doi:10.1016/j.jmb.2006.01.080 J. Mol. Biol. (2006) 357, 1437–1448

JMB

Available online at www.sciencedirect.com

SCIENCE DIRECT®

ELSEVIER

Binding Properties of Pyochelin and Structurally Related Molecules to FptA of *Pseudomonas aeruginosa*

Gaëtan L. A. Mislin[1], Françoise Hoegy[1], David Cobessi[1], Keith Poole[2] Didier Rognan[3] and Isabelle J. Schalk[1]*

[1]*Métaux et Microorganismes: Chimie, Biologie et Applications, UMR 7175-LC1 Institut Gilbert-Laustriat CNRS, Université Louis Pasteur (Strasbourg 1), ESBS, Bld Sébastien Brant, F-67413 Illkirch, Strasbourg, France*

[2]*Department of Microbiology and Immunology, Queen's University, Kingston, Ont. Canada K7L3N6*

[3]*Département de Pharmacochimie de la Communication Cellulaire, UMR7175-LC1 Institut Gilbert-Laustriat CNRS, Université Louis Pasteur (Strasbourg 1), Faculté de Pharmacie 74, route du Rhin BP 60024 67401 Illkirch Graffenstaden Cedex, France*

**Corresponding author*

Pyochelin (Pch) is a siderophore that is produced in iron-limited conditions, by both *Pseudomonas aeruginosa* and *Burkholderia cepacia*. This iron uptake pathway could therefore be a target for the development of new antibiotics. Pch is (4′*R*,2″*R*/*S*,4″*R*)-2′-(2-hydroxyphenyl)-3″-methyl-4′,5′,2″,3″,4″,5″-hexahydro-[4′,2″]bithiazolyl-4″-carboxylic acid, and has three chiral centres located at positions C4′, C2″ and C4″. In *P. aeruginosa*, this siderophore chelates iron in the extracellular medium and transports it into the cells *via* a specific outer membrane transporter FptA. Docking experiments using the X-ray structure of FptA–Pch–Fe showed that iron-loaded or unloaded Pch diastereoisomers could bind to FptA. This was confirmed by *in vivo* binding assays. These binding properties and the iron uptake ability were not affected by removal of the C4′ chiral centre. After removal of both the C4′ and C2″ chiral centres, the molecule still bound to FptA but was unable to transport iron. The overall binding mode of this iron-complexed analogue was inverted. These findings describe the first antagonist of the Pch/FptA iron uptake pathway. Pch also complexes with iron in conjunction with other bidentate ligands such as cepabactin (Cep) or ethylene glycol. Docking experiments showed that such complexes bind to FptA *via* the Pch molecule. The mixed Pch–Fe–Cep complex was also recognized by FptA, having an affinity intermediate between that for Pch_2–Fe and Cep_3–Fe. Finally, the iron uptake properties of the different Pch-related molecules suggested a mechanism for FptA–Pch–Fe complex formation similar to that of the FpvA/Pvd uptake system. All these findings improve our understanding of specificity of the interaction between FptA and its siderophore.

Keywords: siderophore; outer membrane transporter; iron uptake; pyochelin; cepabactin

Introduction

Pseudomonas aeruginosa and *Burkholderia* (ex *Pseudomonas*) *cepacia* are Gram-negative bacteria found in many environments. These bacteria are highly pathogenic for individuals having compromised immune systems and are the cause of chronic lung infections in about 90% of individuals suffering from cystic fibrosis.[1,2] Septicaemic infections involving these organisms have a poor prognosis despite recent advances in anti-microbial chemotherapy.[3] Like all bacterial pathogens, *P. aeruginosa* and *B. cepacia* must acquire iron, an essential nutrient, from the host to grow and establish infections. In iron-poor environments, many bacteria produce highly efficient and specific Fe(III)-chelating agents called siderophores.[4–6] Many clinical isolates of *P. aeruginosa* and *B. cepacia* respond to iron-limiting growth conditions by producing the siderophore pyochelin (Pch).[7–10] This compound is released into the extracellular environment where it complexes with iron and delivers it to the bacterial cell *via* a specific outer membrane receptor, FptA in the case of *P. aeruginosa*.[11] A number of reports have shown a

Abbreviations used: Pch, pyochelin; Pvd, pyoverdine; Cep, cepabactin; OMT, outer membrane transporter; CCCP, carbonyl cyanide *m*-chlorophenylhydrazone; pmf, proton motive force.

E-mail address of the corresponding author: schalk@esbs.u-strasbg.fr

correlation between Pch production and the virulence of *P. aeruginosa*. Pch stimulates bacterial growth in murine infections[12] and efficiently removes iron from transferrin.[13] Pch–Fe(III) can also catalyse hydroxyl radical formation and may play a role in the tissue destruction associated with *P. aeruginosa* infections.[14–16] Finally, mutant strains with defects in Pch-mediated Fe(III) transport were found to be considerably less virulent than wild-type *P. aeruginosa* strains.[17]

Proton and ^{13}C NMR spectroscopy and high-resolution mass spectrometry, and comparisons with synthesised Pch[18–21] has shown Pch to be (4′*R*,2″*R*/*S*,4″*R*)-2′-(2-hydroxyphenyl)-3″-methyl-4′,5′,2″,3″,4″,5″-hexahydro-[4′,2″]bithiazolyl-4″-carboxylic acid, having three chiral centres located at positions C4′, C2″ and C4″. Although there is partial stereocontrol during chemical synthesis, Pch is normally obtained as a mixture of the four diastereoisomers Pch **1** (4′*R*,2″*R*,4″*R*), Pch **2** (4′*R*,2″*S*,4″*R*), neoPch **3** (4′*S*,2″*R*,4″*R*) and neoPch **4** (4′*S*,2″*S*,4″*R*) (Figure 1). The influence of the C4′ and C2″ chiral centres on the biological properties when binding to the FptA receptor have never been described.

Pch is synthesised by the bacteria from salicylate and two molecules of cysteine *via* a thiotemplate mechanism.[22,23] The genes for Pch biosynthesis are clustered in two operons, *pchDCBA* and *pchEFGHI*, on the *P. aeruginosa* chromosome, next to the Pch receptor gene *fptA*.[24,25] Pch biosynthesis is autoregulated by a positive-feedback loop, requiring the transcriptional regulator PchR.[24] The autoinduction mechanism is not completely understood, but is thought to involve an initial interaction of Pch with its outer membrane receptor, FptA, followed by activation of the transcriptional regulator PchR, which turns on the transcription of the Pch biosynthetic operons *pchDCBA* and *pchEFGHI*.[25,26] When the cells have accumulated an excess of iron, the Fur repressor is activated, switching off the Pch biosynthetic gene expression.[24–27]

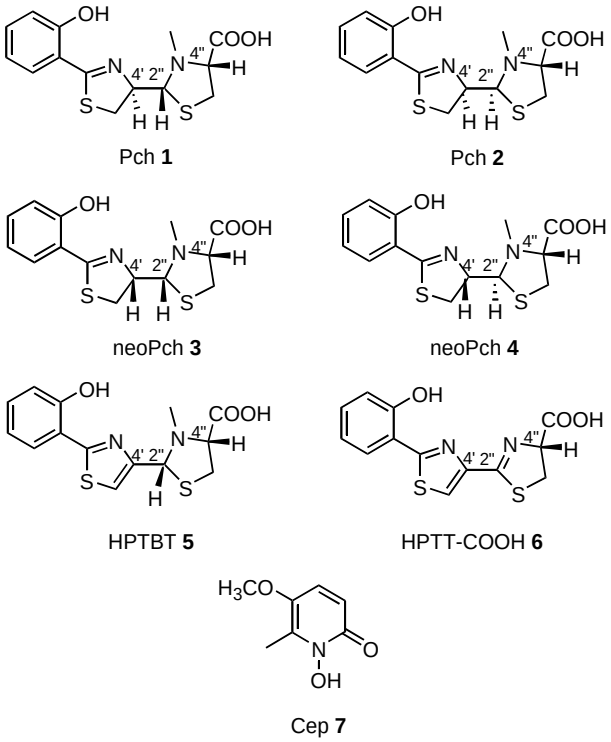

Figure 1. Structures of FptA ligands. Pch **1** to **4** are the different diastereoisomers of synthetic Pch, but only Pch **1** and Pch **2** are the naturally produced siderophores of *P. aeruginosa*. In our study, Pch **1**/**2** is mainly Pch **1** and **2** (proportions of Pch **1**/Pch **2**/neoPch **3**/neoPch **4**: 4/3/2/1) and neoPch **3**/**4** is mainly neoPch **3** and neoPch **4** (proportions of Pch **1**/Pch **2**/neoPch **3**/neoPch **4**: 2/1/4/3). In the presence of a metal ion, Pch **2** isomerises into Pch **1**[7,21] and neoPch **4** into neoPch **3**.

Pch is able to chelate Fe(III) with a 2:1 or 1:1 (Pch:Fe(III)) stoichiometry, depending on the presence or not of an excess of siderophore.[8,18,19,28] This siderophore has a poor water-solubility and its Fe(III) affinity was determined in methanol as $2\times 10^5\ M^{-1}$,[18] which is low compared to other siderophores. It is possible that in aqueous solution at physiological pH values the affinity for iron may be higher. Pch also chelates Zn(II), Cu(II), Co(II), Mo(VI) and Ni(II) ions[29] and Pch may also mobilize these metals ions and deliver them to the cell.

The structure of the Pch outer membrane receptor, FptA, from *P. aeruginosa* PAO1, loaded with ferric-Pch, has recently been determined.[30] The structure of the protein is typical of this class of transporter:[31–36] a transmembrane 22 β-stranded barrel occluded by a N-terminal domain containing a mixed four-stranded β-sheet (Figure 2). The Pch binding pocket is principally composed of hydrophobic and aromatic residues, consistent with the hydrophobicity of this siderophore.[30] One Pch molecule complexed with iron was found in the binding site, thus providing the first three-dimensional structure of this siderophore. Pch provides a tetradentate coordination of iron, and ethyleneglycol, which is not specifically recognized by the protein, provides a bidentate coordination.[30] Another 1:1:1 complex between Pch (tetradentate), cepabactin (Cep, a bidentate siderophore) and iron(III) was isolated and characterized from *B. cepacia* culture medium.[37]

As Pch is almost always found in *P. aeruginosa* and *B. cepacia* species, it could be assumed that most of these strains have a common or very closely related Pch outer-membrane receptor, called FptA. Also, as iron is essential for these pathogenic organisms, FptA could be a promising target for new antibiotic design or could be used, for example, to transport antibiotics into the cells using a Trojan horse strategy.[38–40] The development of such strategies requires knowledge of the recognition mechanism by FptA of Pch and ferric-Pch and a better understanding of the structure–activity relationships between Pch analogues and FptA. Therefore, we have investigated the binding and iron uptake properties of FptA with the four diastereoisomers of synthetic Pch, with other Pch

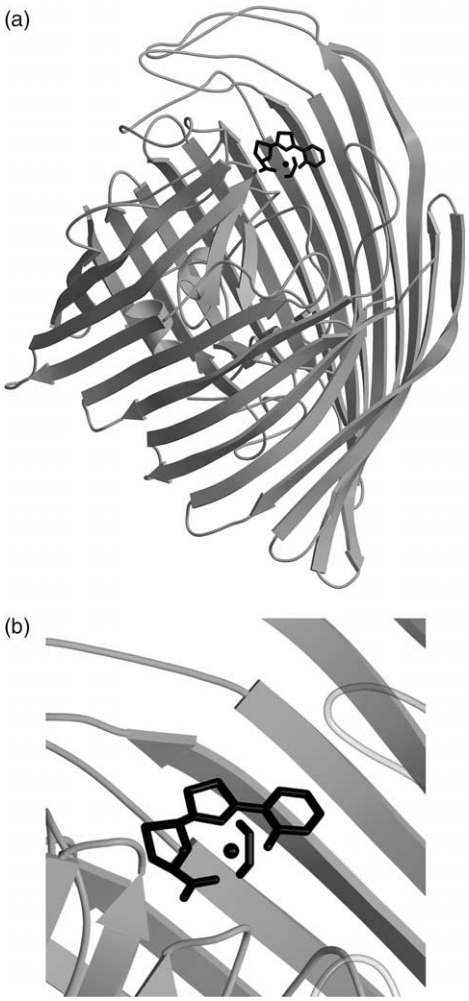

Figure 2. The FptA–Pch–Fe structure (PDB entry 1XKW).[57] (a) View of the overall structure. (b) View of the Pch–Fe binding site. The Pch and ethylene glycol molecules are shown as sticks and the iron ion is shown as a sphere.

analogues, with the Pch–Fe–Cep complex and with Cep_3–Fe. We clearly show that the different diastereoisomers of synthetic Pch (compounds Pch **1**, Pch **2**, neoPch **3** and neoPch **4**; Figure 1) can bind to FptA and transport iron. These biological properties are also not noticeably affected by removing the C4′ chiral centre of Pch (Pch analogue HPTBT **5**; Figure 1). When the C4′ and C2″ chiral centres are removed (HPTT-COOH **6**; Figure 1), the ferric-Pch analogue still binds to FptA but is not transported. All these *in vivo* results are consistent with docking experiments based on the structure of FptA. They suggest that the Pch binding site on FptA recognises ferric HPTT-COOH **6** but that the binding mode is completely different compared to the natural siderophore. This study also shows that FptA can recognise mixed complexes such as Pch–Fe–Cep *via* the Pch face, and Cep_3–Fe. Finally, we provide some evidence for the presence of a Cep outer-membrane transporter coupled to the proton motive force in *P. aeruginosa*, although this micro-organism is not able to synthesize this siderophore.

Results

Binding of Pch analogues

The specificity of iron uptake in Gram-negative bacteria is regulated by outer membrane transporters (OMTs). These are highly specific for one or a few siderophores. Pch is synthesized in the laboratory as a mixture of the four diastereoisomers Pch **1** (4′*R*,2″*R*,4″*R*), Pch **2** (4′*R*,2″*S*,4″*R*), neoPch **3** (4′*S*,2″*R*,4″*R*) and neoPch **4** (4′*S*,2″*S*,4″*R*) (Figure 1). We have investigated for the first time the influence of the chiral centres on the biological properties when binding to the FptA receptor. We have previously shown that the FptA receptors expressed at the cell surface in a Pch-producing strain are loaded with iron-free Pch.[41] Therefore, we used a Pch and Pvd-deficient strain (PAD07) for the binding assay to avoid competition with an endogenous siderophore.

The Pch diastereoisomer mixtures used were Pch **1**/**2**, which is mainly Pch **1** and Pch **2** (proportions of Pch **1**/Pch **2**/neoPch **3**/neoPch **4**:4/3/2/1), and neoPch **3**/**4**, which is mainly neoPch **3** and neoPch **4** (proportions of Pch **1**/Pch **2**/neoPch **3**/neoPch **4**:2/1/4/3). Isolation of one stereoisomer from the other three is arduous and often leads to enriched fractions of the expected diastereoisomers contaminated by one or several of the other Pch isomers. In the presence of a metal ion, Pch **2** isomerises into Pch **1**[7,21] and neoPch **4** isomerises into neoPch **3**. Only the epimers Pch **1** and Pch **2** are naturally produced by *P. aeruginosa* and *B. cepacia*.[8] (Pch **1**/**2**)$_2$–Fe and (neoPch **3**/**4**)$_2$–Fe are recognised with similar affinities by FptA (Figure 3(a); Table 1). FptA was also able to bind the apo form of Pch **1**/**2** and neoPch **3**/**4** with a tenfold difference in the affinities compared to the ferric forms (Table 1). Compared to (Pch **1**/**2**)$_2$–Fe, there was a threefold decrease in the affinity of (HPTBT **5**)$_2$–Fe, in which the C4′ chiral centre of the siderophore was removed, and a sixfold decrease in the affinity of (HPTT-COOH **6**)$_2$–Fe, in which the C2″ chiral centre was removed, for FptA (Table 1).

According to the FptA–Pch–Fe structure, one molecule of Pch is sufficient for the recognition of the ferric-siderophore by the transporter (Figure 1).[30] To confirm this observation, the binding properties of Pch–Fe–Cep isolated from *B. cepacia* culture media[37] and of Cep_3–Fe have been investigated. We found that the Pch–Fe–Cep and Cep_3–Fe complexes were recognized by FptA with affinities of 45($\pm$8.5) nM and 435($\pm$8.5) nM, respectively (Table 1; Figure 3(b)). Surprisingly, the FptA receptor was also able to bind the siderophore Cep, which is structurally different from Pch, but with 200 times lower affinity than for (Pch **1**/**2**)$_2$–Fe. The mixed Pch–Fe–Cep complex was recognized by FptA with an intermediate affinity between (Pch **1**/**2**)$_2$–Fe and Cep_3–Fe (Table 1; Figure 3(b);) 20 times lower compared to (Pch **1**/**2**)$_2$–Fe). Therefore, it is probably the Pch in the

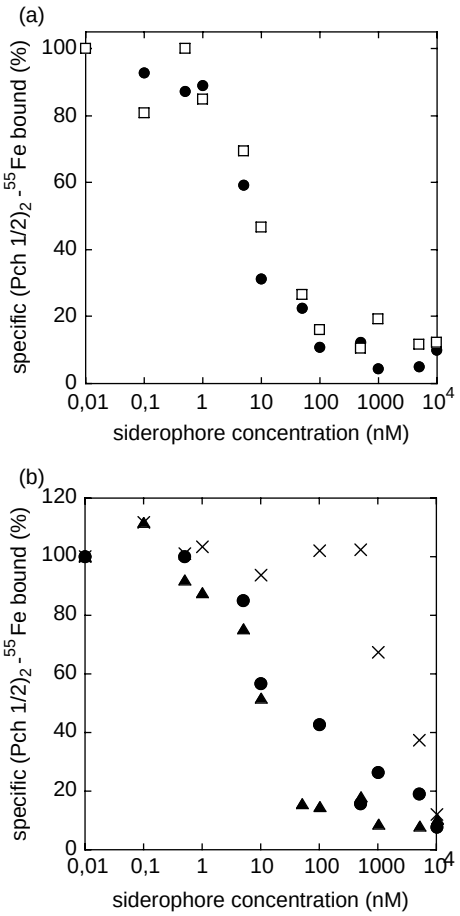

Figure 3. Competition experiments. Competition by unlabelled (Pch **1**/**2**)$_2$–Fe, (neoPch **3**/**4**)$_2$–Fe, Pch–Fe–Cep and Cep$_3$–Fe for the binding of (Pch **1**/**2**)$_2$–^{55}Fe to FptA *in vivo*. Experiments were carried out as described in Materials and Methods in the presence of 1 nM (Pch **1**/**2**)$_2$–^{55}Fe, Pch and Pvd-deficient PAD07 cells at A_{600} of 0.3, and various concentrations of (Pch **1**/**2**)$_2$–Fe ((a) and (b), ●), (neoPch **3**/**4**)$_2$–Fe ((a), □); Pch–Fe–Cep ((b), ▲) and Cep$_3$–Fe ((b), X). The experiments were repeated three times with comparable results.

mixed complex that interacts with the FptA binding pocket, with Cep not being essential for recognition by the transporter.

Table 1. Inhibition constants (K_i)

Siderophores	K_i (nM)
Pch **1**/**2**	26.9 ± 0.7
(Pch **1**/**2**)$_2$–Fe	2.2 ± 0.5
neoPch **3**/**4**	40.6 ± 4.0
(neoPch **3**/**4**)$_2$–Fe	3.1 ± 0.2
(HPTBT **5**)$_2$–Fe	9.8 ± 3.5
(HPTT-COOH **6**)$_2$–Fe	27 ± 5
Pch–Fe–Cep	45 ± 8.5
Cep$_3$–Fe	435 ± 9.5

K_i values were determined from competition experiments against (Pch **1**/**2**)$_2$–^{55}Fe. PAD07 (A_{600} = 0.3) cells were incubated with 1 nM (Pch **1**/**2**)$_2$–^{55}Fe and increasing concentrations of the studied siderophore. The experiment was carried out at 0 °C to avoid iron uptake.

Iron transport properties of Pch analogues

The iron uptake efficiencies in *P. aeruginosa* PAO1 of the Pch diastereosiomers, the related Pch compounds and Cep–Fe were estimated using ^{55}Fe (Figure 4). We repeated all the experiments in the presence of the protonophore CCCP, in which iron uptake is inhibited, and in the absence of cells. We have previously shown that the FptA receptors expressed at the cell surface in a Pch-producing strain are loaded with iron-free Pch.[41] This FptA-bound Pch may play an essential role in the iron uptake mechanism and may be involved in the formation of iron-loaded FptA, as suggested for the iron uptake transporters in *Aeromonas hydrophila*.[42] We used the Pch and Pvd-deficient PAD07 strain to evaluate the importance of this FptA-bound Pch in the iron uptake process (Figure 4).

(Pch **1**/**2**)$_2$–Fe and (neoPch **3**/**4**)$_2$–Fe were transported with similar efficiencies in both the siderophore-producing *P. aeruginosa* PAO1 cells and the Pch and Pvd-deficient PAD07 cells (Figure 4(a)). HPTBT **5** (no C4′ chiral centre) transported iron with the same efficiency as Pch **1**/**2** (Figure 4(b)). Iron-loaded HPTT-COOH **6** (no C4′ and C2″ chiral centres) bound to FptA (Table 1) but there was no iron uptake (Figure 4(b)). Therefore, structural differences between HPTT-COOH **6** and the other molecules tested affect iron uptake rates in both *P. aeruginosa* strains. As we obtained the same results with both Pch-producing and Pch-deficient cells (Figure 4), it would appear that the endogenous Pch bound to FptA at the outer membrane is not involved in the iron uptake process or in the formation of iron-loaded FptA.

Cep transported iron with the same efficiency as Pch **1**/**2** in both the Pch-producing PAO1 cells and the Pch and Pvd-deficient PAD07 cells (Figure 4(c)). As no ^{55}Fe uptake occurred at 0 °C in the presence of CCCP, the iron uptake *via* Cep is proton motive force (pmf)-dependent. We repeated the experiment in an *fptA* and Pvd-deficient strain (K2388) to determine whether Cep$_3$–Fe uptake occurs *via* FptA or *via* another receptor. We observed a pmf-dependent ^{55}Fe uptake (Figure 5), indicating that there must be an unknown specific Cep$_3$–Fe OMT in *P. aeruginosa*. This OMT cannot transport (Pch **1**/**2**)$_2$–^{55}Fe (Figure 5). The presence in the *Pseudomonas* strains used here of this unknown Cep OMT, means that we were unable to conclude our studies of FptA transport of Cep$_3$–Fe. Finally, we could not test the iron uptake properties of the Pch–^{55}Fe–Cep complex because of the difficulty of preparing the radioactive form of this complex.

Ligand docking

We carried out docking experiments using the X-ray structure of FptA loaded with (Pch **1**)–Fe[30] to better understand the interaction mechanism of the FptA binding site with the seven Pch diastereoisomers and analogues (Figure 1). The program GOLD (genetic optimisation for ligand docking),[43] a

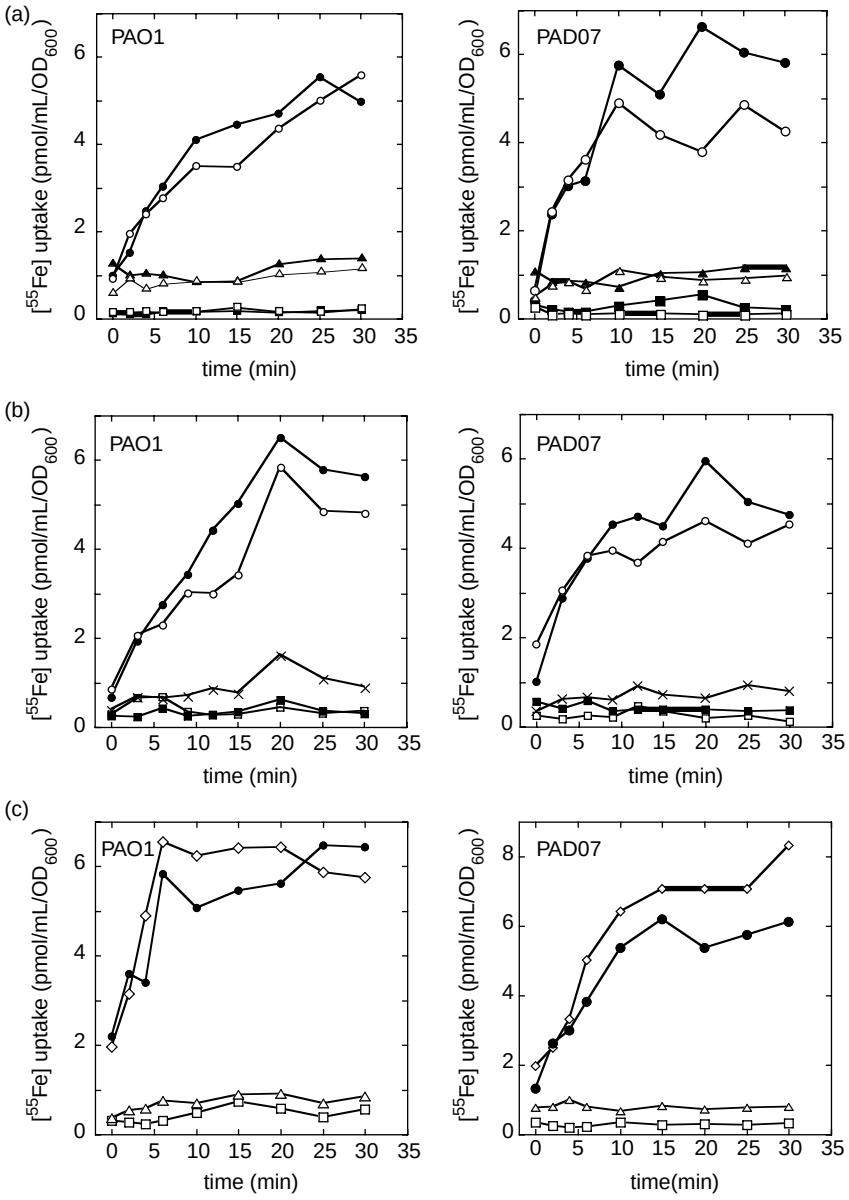

Figure 4. ^{55}Fe uptake by *P. aeruginosa* strains PAO1 and PAD07. (a) *P. aeruginosa* PAO1 (left panel) and PAD07 (right panel) cells at an A_{600} of 1 were incubated at 37 °C for 15 min in 50 mM Tris–HCl (pH 8.0) before the transport assays were started by the addition of (Pch **1**/**2**)$_2$–^{55}Fe (●) or (neoPch **3**/**4**)$_2$–^{55}Fe (○). Aliquots (100 µl) of the cell suspensions were removed at different times, filtered and the retained radioactivity was counted. The experiments were repeated in the presence of 200 µM CCCP (▲ for (Pch **1**/**2**)$_2$–^{55}Fe and △ for (neoPch **3**/**4**)$_2$–^{55}Fe) and in the absence of cells (□ for (Pch **1**/**2**)$_2$–^{55}Fe and □ for (neoPch **3**/**4**)$_2$–^{55}Fe). For each uptake experiment, the radiolabelled analogue was used at a concentration of 10 nM. (b) The experiment was repeated at 37 °C in the presence of (Pch **1**/**2**)$_2$–^{55}Fe (●), (HPTBT **5**)$_2$–^{55}Fe (○) or (HPTT-COOH **6**)$_2$–^{55}Fe (X), and in the presence of 200 µM CCCP for (HPTBT **5**)$_2$–^{55}Fe (□) or (HPTT-COOH **6**)$_2$–^{55}Fe (■). For each uptake experiment, the radiolabelled analogue was used at a concentration of 10 nM. (c) The experiment was repeated at 37 °C in the presence of (Pch **1**/**2**)$_2$–^{55}Fe (●) or Cep$_3$–^{55}Fe (◇), and for Cep$_3$–^{55}Fe, in the presence of 200 µM CCCP (△) and in the absence of cells (□). Again, for each uptake experiment, the radiolabelled analogue was used at a concentration of 10 nM. All the experiments shown on the same graph were carried out on the same batch of cells.

genetic algorithm for docking flexible ligands into protein binding sites was used to dock all the ligands investigated here. Using automated docking, we obtained a (Pch **1**)$_2$-Fe conformation very close to that of its X-ray structure (rmsd of 0.3 Å from the heavy atoms) and with a high GOLDscore of 63.8 (Figure 6(a); Table 2). Iron complexation by neoPch **3** did not alter the binding mode to FptA with respect to the X-ray conformation of (Pch **1**)$_2$–Fe (Figure 6(a); Table 2). The bound conformation of iron-free Pch **1** was close to that of the X-ray conformation of bound Pch **1**–Fe, with an rmsd of 1.2 Å (Figure 6(b)). For the docking of iron-free Pch **2** in the FptA binding site (Figure 6(c)), the phenol moiety adopted the same conformation in the hydrophobic part of the binding site, but unlike the case for Pch **1**, the carboxylate group was no longer H-bonded to the L116 and/or L117 backbone nitrogen atoms, but was interacting with the polar side-chains of N703 and R705. We observed a similar conformation with iron-free neoPch **4**, but with the establishment of a single H-bond to R705 (Figure 6(c)). For the four diastereoisomers investigated, the docking scores were very similar (GOLDscore ranging from 44.9 to 53.1; Table 2) but were lower than for the ferric complexes of Pch **1** and neoPch **3**. The synthetic thiazole analogue, HPTBT$_2$-Fe **5**, also exhibited the same binding modes (Figure 6(d)). Although the phenol group was rotated with respect to the thiazole moiety, the two five-membered rings were similarly embedded into the binding site. The carboxylic acid was H-bonded to the L116 backbone nitrogen atom, with a docking score of 50.94 (Table 2). The iron-complexed HPTT-COOH **6** docked only when the molecule was inverted in the binding site (Figure 6(d)). The phenol moiety H-bonded to the L117 backbone nitrogen atom whereas the

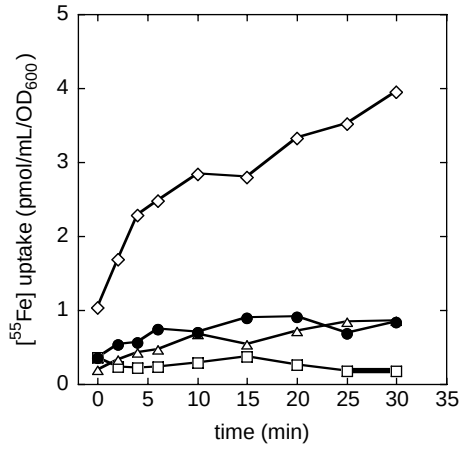

Figure 5. ^{55}Fe uptake by Pvd and *fptA*-deficient cells. Pvd and *fptA*-deficient K2388 cells at an A_{600} of 1 were incubated at 37 °C for 15 min in 50 mM Tris–HCl (pH 8.0) before the transport assays were started by the addition of 10 nM (Pch **1**/**2**)$_2$–^{55}Fe (●) or Cep$_3$–^{55}Fe (◇). Aliquots (100 μl) of cell suspensions were removed at different times, filtered and the retained radioactivity was counted. The experiment was repeated with Cep$_3$–^{55}Fe in the presence of 200 μM CCCP (△) and in the absence of cells (□).

carboxylic acid bulged out of the binding cavity. This inverted binding mode did not affect the observed docking score (Table 2) because the main hydrophobic interactions with M271, F114, L117, F358 and Y356 were conserved (Figure 6(d)). For both synthetic Pch analogues HPTBT **5** and HPTT-COOH **6**, a much higher proportion of the ligand's surface was accessible to solvent (Table 2) than for the diastereoisomers.

The Pch **1**–Cep–Fe ternary complex was predicted to bind in a similar way to Pch$_2$–Fe, with the Cep molecule simply replacing ethylene glycol in the hexadentate coordination (Figures 2 and 6(e)). However, the good docking score should be weighted to take into account the higher mass of this ternary ligand and its higher accessibility to water when bound to the receptor (Table 2). Lastly, (Cep)$_3$–Fe could only be docked with a large steric hindrance in the current FptA structure, due to significant steric bumps with I116, T143, M271 and W702 (Table 2; Figure 6(f)).

Discussion

Pch is a siderophore that is produced under iron-limited conditions by many pathogenic strains of *P. aeruginosa* and *B. cepacia*. This natural molecule contains three chiral centres, but only the Pch **1** and Pch **2** (Figure 1) are produced by the bacteria *via* a stereo-controlled multi-enzymatic process.[22] Organic synthesis of Pch gives a mixture of the four diastereoisomers Pch **1**, Pch **2**, neoPch **3** and neoPch **4** (Figure 1) in varying proportions depending on whether D-cysteine or L-cysteine is used as a building block. The total synthesis of Pch from D-cysteine gives a mixture of isomers referred to Pch **1**/**2**, comprising mainly diastereoisomers Pch **1** and Pch **2** (proportions of Pch **1**/Pch **2**/neoPch **3**/neoPch **4**: 4/3/2/1).[7] Starting with L-cysteine gives neoPch **3**/**4**, comprising mainly neoPch **3** and neoPch **4** (proportions of Pch **1**/Pch **2**/neoPch **3**/neoPch **4**: 2/1/4/3).[7,20] In the presence of a metal ion, Pch **2** isomerises into Pch **1**[7,20] and neoPch **4** isomerises into neoPch **3**. This suggests that there is a metal-driven template effect giving a *cis* H2″-H4″ relationship that is necessary for optimal ferric ion tetra-coordination by the siderophore.

During iron uptake in *P. aeruginosa*, the ferric-Pch **1** is recognized by the specific transporter, FptA.[11] The high-resolution X-ray structure of FptA loaded with Pch **1**–Fe has been determined[30] and shows an overall folding structure similar to that of other siderophore receptors. The C terminus is folded into a transmembrane 22 β-stranded barrel, which is occluded by the N-terminal domain, called the plug or cork domain. The Pch binding pocket comprises principally hydrophobic and aromatic residues, which is consistent with the hydrophobicity of Pch. In this structure, the ferric ion is hexa-coordinated by four atoms from the Pch (the nitrogen atoms of the thiazolin and thiazolidin rings, and the oxygen atoms of the phenolate and carboxylate groups) and the two oxygen atoms from ethylene glycol, with a 1:1:1 stoichiometry.[30] The observed diastereoisomer of Pch in this FptA structure is Pch **1**: (4′*R*,2″*R*,4″*R*)-2′-(2-hydroxyphenyl)-3″-methyl-4′,5′,2″,3″,4″,5″-hexahydro-[4′,2″]bithiazolyl-4″-carboxylic acid.[30] Our docking experiments predict that the four Pch disatereoisomers (Figure 1) should interact with the FptA binding site. We validated the automated docking procedure by docking ferric Pch **1** into the X-ray structure of the FptA binding site.[30] The top-ranked conformation was very similar to the X-ray conformation (rmsd of 0.3 Å) suggesting that Gold can properly dock this ligand with the receptor (Figure 6(a)). Ferric Pch **1** is completely rigid due to the iron atom, which simplifies the docking process. However, the very good docking score we obtained suggests that our docking parameters can discriminate realistic configurations from unrealistic configurations (Table 2). The binding of iron-free Pch **1** and neoPch **3** was not significantly altered (Figure 6(b)). This is consistent with close affinities (tenfold difference) of FptA for iron-free and (Pch **1**/**2**)$_2$–Fe, 26.9 nM and 2.2 nM, respectively (Table 1).[41] In all Pch diastereoisomers, the phenol moiety is predicted to bind similarly to a hydrophobic subsite (Y356, F358, A144, L117) and the two five-membered heterocycles face the central non-polar part of the binding site (M271, Y334, W702). However, the carboxylate moiety is proposed to H-bond to two different polar environments, the L116 and L117 backbone nitrogen atoms or the N703 and R705 side-chains (Table 2; Figure 6(a)–(c)). The ligands are much more flexible in the absence of an

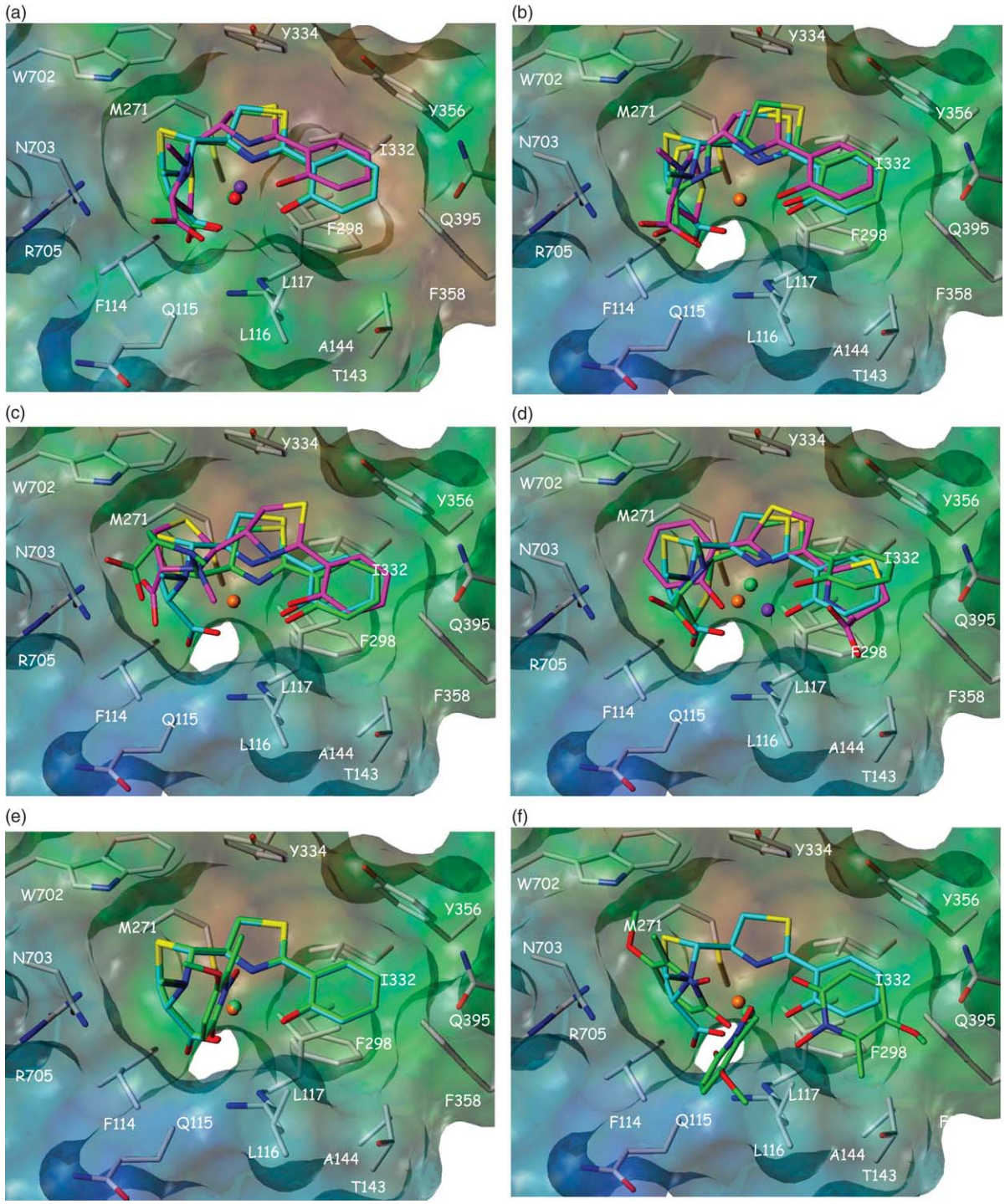

Figure 6. Predicted binding modes of the FptA ligands 1–7. Non-carbon ligand atoms are coloured as follows: oxygen, red; nitrogen, blue; sulphur, yellow. The molecular surface of the FptA binding site (white sticks) was rendered using the SYBYL implementation of MOLCAD[58] and colour-coded by hydrophobicity (brown→blue: hydrophobic→ hydrophilic). FptA contacting residues are labelled at the C^{α} atom. (a) Overlay of the X-ray structure of Pch **1** (cyan carbon atoms), predicted pose of iron-bound Pch **1** (green carbon atoms), and of predicted pose of iron-bound neoPch **3** (magenta carbon atoms). Fe ions are shown as orange, green-blue and purple balls when bound to Pch **1** (X-ray), Pch **1** (predicted) and neoPch **3**, respectively. (b) Overlay of X-ray structure of iron-bound Pch **1** (cyan carbon atoms) with the predicted pose of iron-free Pch **1** (green carbon atoms) and of iron-free neoPch **3** (magenta carbon atoms). The Fe^{3+} is displayed by an orange ball. (c) Overlay of the X-ray structure of iron-bound Pch **1** (cyan carbon atoms) with the predicted poses of iron-free Pch **2** (green carbon atoms) and iron-free neoPch **4** (magenta carbon atoms). The Fe^{3+} is shown as an orange sphere. (d) Overlay of the X-ray structure of iron-bound Pch **1** (cyan carbon atoms) with the predicted poses of iron-bound HPTBT **5** (green carbon atoms) and HPTT-COOH **6** (magenta carbon atoms). Fe ions are shown as orange, green-blue and purple balls when bound to Pch **1** (X-ray), HPTBT **5** and HPTT-COOH **6**, respectively. (e) Overlay of the X-ray pose of iron-bound Pch **1** (cyan carbon atoms) with the predicted pose of the ternary ligand Pch

Table 2. Predicted binding mode of FptA ligands by Gold automated docking

Ligand	GOLDscore[b]	rmsd[c]	H-bonds[a]				BSA[d]
			L116:N	L117:N	N703:ND2	R705:NH2	
(Pch **1**)$_2$–Fe	63.81	0.30		×			97.5
Pch **1**	49.35	1.22	×	×		×	97.0
Pch **2**	44.96				×		88.0
(neoPch **3**)$_2$–Fe	52.57		×				94.5
neoPch **3**	53.12		×		×		97.1
neoPch **4**	49.60				×	×	100.0
(HPTBT **5**)$_2$–Fe	50.94		×		×		50.8
(HPTT-COOH **6**)$_2$–Fe	49.17			×			50.0
(Pch **1**)$_2$–Fe-**7**	57.38			×			57.8
(Cep)$_3$–Fe	6.65		×	×			70.8

[a] Possible H-bonds are indicated by a cross.
[b] GOLDscore is the fitness function of the GOLD program,[56] which quantifies protein–ligand interactions according to four terms: protein–ligand H-bond interaction energy; protein–ligand van der Waals interaction energy; ligand internal van der Waals energy; ligand torsional strain energy.
[c] Root-mean-square deviations (in Å) of the heavy atoms from the X-ray configuration of (Pch **1**)$_2$–Fe.
[d] Buried surface area (in percentage of the total surface) of the FptA-bound ligand.

iron ion, although the proposed binding modes of the iron-free ligands are often similar to those of the equivalent iron complexes (Table 2; Figure 6(b) and (c)). However, their binding conformations differ, resulting in different abilities to complex iron. Pch **1** and neoPch **3** adopt the same bound conformation irrespective of the presence of iron (Figure 6(b)), whereas the receptor-bound conformation of Pch **2** and neoPch **4** are incompatible with strong metal chelation because of a *trans* relationship between H2″ and H4″ protons repelling the carboxylic acid moiety far from the iron coordination sphere (Figure 6(c)).

Our experimental data show that both (Pch **1**/**2**)$_2$–Fe and (neoPch **3**/**4**)$_2$–Fe have the same affinities for FptA (Table 1; Figure 3) and are able to transport iron with the same efficiencies (Figure 4(a)). FptA is also able to bind the apo-forms of Pch **1**/**2** and neoPch **3**/**4** (Figure 3(b)). These results are consistent with the high scores for the two ferric complexes, the apo forms of Pch **1** and neoPch **3** (Table 2; Figure 6(a) and (b)) and strongly suggest that FptA is able to bind Pch **1**, neoPch **3**, (Pch **1**)$_2$–Fe and (neoPch **3**)$_2$–Fe.

NeoPch **3** differs from Pch **1** only by the stereochemistry of the C4′ chiral centre. When this stereocentre was removed by replacing the thiazolin moiety by a thiazole ring in HPTBT **5**, we observed only a slight decrease in the affinity for FptA (Table 1) and iron transport properties similar to Pch **1**/**2** (Figure 4(b)). Inversion of the chiral centres in Pch or the synthetic HPTBT **5** compound is accommodated by the carboxylate group H-bonding to one of the two polar environments (Table 2; Figure 6(d)). When both the C4′ and C2″ chiral centres are removed (HPTT-COOH **6**), the ferric-siderophore becomes more rigid, its affinity for FptA is decreased (tenfold compared to (Pch **1**/**2**)$_2$–Fe; Table 1) and it no longer transports iron (Figure 4(b)). This inhibition of iron uptake occurs *via* an as yet unknown mechanism. Although (HPTT-COOH **6**)$_2$-Fe could be docked into the binding site with a score very similar to Pch diastereoisomers (Table 2), there is a complete inversion of the binding mode with FptA (Figure 6(d)). The position of the Fe^{3+} in the FptA–(HPTT-COOH **6**)$_2$–Fe complex has not changed significantly with respect to that observed in the X-ray structure of FptA in complex with ferric-Pch (distance of 1.56 Å). It is therefore likely that the position of the HPTT-COOH **6** ligand is no longer suitable to promote iron transport because of steric and/or electrostatic hindrance. This inversion may be the origin of the unusual biological properties of HPTT-COOH **6**.

Analysis of the published FptA structure shows that Pch can coordinate iron with another bidentate molecule, such as ethylene glycol (Figure 2), in a 1:1:1 stoichiometry, and that the complex is recognized by the transporter.[30] A complex composed of one iron(III) ion, one Cep and one Pch has been isolated[37] from growth medium of *B. cepacia*, which also produces other siderophores.[44] Our competition experiments show that this complex can bind to FptA with an affinity intermediate between that of (Pch **1**/**2**)$_2$–Fe and Cep$_3$–Fe (Table 1). Our docking experiments and the FptA structure (Figure 2)[30] show that the FptA binding

1-iron-Cep (green carbon atoms). Fe ions are shown as orange and green-blue balls when bound to Pch **1** (X-ray) and ligand Pch **1**–iron–Cep, respectively. (f) Overlay of the X-ray pose of iron-bound Pch **1** (cyan carbon atoms) with the predicted pose of the iron–Cep complex (green carbon atoms). Fe ions are shown as orange and green-blue balls when bound to Pch **1** (X-ray) and iron–Cep complex, respectively.

site recognises the Pch in these mixed ferric complexes (Figure 6(e)). One molecule of Pch per ferric complex seems sufficient to be recognized by the FptA transporter, although we are unable to say whether one molecule of Pch per ferric complex is sufficient for the iron uptake process *via* FptA.

The binding assays show that Cep_3–Fe can bind to FptA with a strongly reduced affinity (200 times lower) compared to (Pch **1**/**2**)$_2$–Fe (Table 1). Attempts to dock Cep_3–Fe to the X-ray structure of FptA yielded very poor docking scores (Table 2) because of steric hindrance with several FptA residues (Figure 6(f)). We have shown (Figure 5) that there must be an as yet unknown specific Cep_3–Fe OMT in *P. aeruginosa*, different from FptA. Since the Cep_3–Fe uptake is pmf-dependent (Figure 5) this unknown receptor is probably like all siderophore OMTs TonB-dependent. Sequence analysis of the complete *P. aeruginosa* genome[45] shows 32 putative TonB-dependent transporters, of which only a few have been characterized. This unknown Cep OMT in the *Pseudomonas* strains used here meant we were unable to conclude our studies on the ability of FptA to transport Cep_3–Fe.

We used both the Pch-producing *P. aeruginosa* PAO1 strain and the Pvd and Pch-deficient PAD07 strain for the iron uptake assays for the different Pch diastereoisomers and analogues. Similar results were observed for both strains (Figures 4 and 5). All the FptA transporters on the cell surface of the wild-type Pch-producing strain were loaded with iron-free Pch under iron-limited conditions.[41] Recognition of iron-free siderophores by TonB-dependent OMTs has been described for FptA,[41] and also for FpvA,[46,47] FecA[35] and FhuA,[41] respectively (the ferric Pvd, ferric dicitrate and ferrichrome outer membrane transporters of *P. aeruginosa* and *Escherichia coli*). This is probably a common feature of many siderophore outer membrane transporters of Gram-negative bacteria. As HPTT-COOH **6** was unable to transport iron in the Pch-producing *P. aeruginosa* PAO1 strain, this FptA-bound Pch cannot aid the iron uptake process. Therefore, the mechanism for forming FptA–Pch_2–Fe during iron uptake cannot be a ligand exchange mechanism, which involves exchanging iron from a ferric siderophore to an iron-free siderophore already bound to the receptor.[42] Instead, the mechanism likely involves displacement of a siderophore on FptA, as shown by us for the FpvA/Pvd uptake system in *P. aeruginosa*.[47–49] The FptA-bound Pch presumably dissociates from FptA in a TonB-dependent process and the extracellular ferric-siderophore then binds to the free binding site on FptA, as shown for FpvA.[47,48]

In conclusion, our data show that all the Pch diastereoisomers are able to bind to FptA. The activity of Pch remains even after removing one chiral centre. However, when two chiral centres are removed, the molecule (HPTT-COOH **6**)$_2$–Fe still binds to the transporter but no iron uptake occurs. Finally, Pch can form mixed complexes with iron and other bidentate ligands, such as Cep and ethylene glycol (Figure 2). These complexes still bind to FptA with a good affinity, *via* the Pch molecule. All these data provide a better understanding of the interaction at the atomic level of Pch and ferric–Pch with the FptA binding site. Knowledge of these structure–activity relationships should aid in the design and synthesis of inhibitors of the ferric–Pch iron uptake pathway.

Materials and Methods

Chemicals

Carbenicillin disodium salt was a gift from SmithKline Beecham (Welwyn Garden City, Herts, UK). The protonophore CCCP (carbonyl cyanide *m*-chlorophenylhydrazone) was purchased from Sigma. $^{55}FeCl_3$ was obtained from Perkin Elmer Life and Analytical Sciences (Billerica, MA, USA) with a specific activity of 81 Ci/g. Pch **1**/**2**–^{55}Fe and other siderophore–^{55}Fe complexes were prepared at concentrations of 1 μM of ^{55}Fe with a siderophore/iron molar ratio of 20:1. The solutions were prepared using a 4.4 mM solution of Pch (in methanol). To 4.5 μl of this solution were added 12.3 μl of a solution of $^{55}FeCl_3$ (81 μM, 81 Ci/g in 0.5 M HCl), obtained by dilution of the stock solution, plus 973 μl of 50 mM Tris–HCl (pH 8.0).

Siderophores and analogues

The Pch diastereoisomer mixtures Pch **1**/**2** and neoPch **3**/**4** (Figure 1) were synthesised from D and L-cysteine, respectively, using a published protocol.[20] Isolation of one stereoisomer from the other three is arduous and often leads to enriched fractions of the expected diastereoisomers contaminated by one or several of the other Pch isomers. The Pch **1** and Pch **2** are naturally produced by *P. aeruginosa* and *B. cepacia*.[7] In the presence of a metal ion, Pch **2** isomerizes into Pch **1**[21,50] and neoPch **4** isomerizes into Pch **3**. HPTBT **5** and HPTT-COOH **6** were synthesised as described (Figure 1)[51]. The mixed iron(III), Cep and Pch complex was isolated from the culture broth of *B. cepacia* ATCC 17754 or ATCC 25416 using a described procedure.[37] Iron-free Cep was obtained by decomplexation of either synthetic[37] or naturally occurring ferric–Cep according to the following procedure: ferric–Cep was dissolved in ethanol (25 μl/mg of ferrisiderophore) to which was added a 10% solution of sodium hydroxide (25 μl/mg of ferrisiderophore). The resulting red solution was gently stirred for 2 h at 20 °C, progressively turning into a light orange coloured solution. The mixture was then adjusted to pH 10 with 1 M HCl and the resulting white precipitate was removed by centrifugation. The supernatant was then extracted overnight (12 h) with dichloromethane. The iron-free siderophore was detected in the aqueous phase with the remaining iron-loaded Cep being detected in the dichloromethane phase. The aqueous phase was then evaporated to dryness under reduced pressure and the resulting light orange solid was triturated several times with acetone. The acetone phases were collected and evaporated to dryness under reduced pressure. Cep concentration was calculated from the resulting crude white powder by UV absorption at $\lambda = 337$ nm ($\varepsilon = 5100\ M^{-1}cm^{-1}$).

Bacterial strains and growth media

Wild-type *P. aeruginosa* strain PAO1[52] and the Pch and Pvd-deficient *P. aeruginosa* strain, PAD07[17] have been described. The Pvd and FptA-deficient strain, K2388, was constructed by disruption of the *fptA* gene of strain PAO6609[53] with an Ω-Tc cartridge according to a published procedure.[53] *Pseudomonas* strains were grown overnight in succinate medium[54] in the presence of 100 μg/ml streptomycin and 50 μg/ml tetracycline for strain PAD07 and 100 μg/ml tetracycline for strain K2388.

Ligand-binding assays using ^{55}Fe

The *in vivo* binding affinity constants (K_i) of (Pch **1**/**2**)$_2$–Fe, (neoPch **3**/**4**)$_2$–Fe, Cep$_3$–Fe and the ferric–Pch analogues and Pch–Fe–Cep complexes to FptA were determined according to the following procedure: PAD07 cells were washed twice with an equal volume of fresh medium and resuspended in 50 mM Tris–HCl (pH 8.0) buffer at an A_{600} of 0.3. The cells were then incubated for 1 h at 0 °C to avoid iron uptake[48] in a final volume of 500 μl with 1 nM of (Pch **1**/**2**)$_2$–^{55}Fe and various concentrations of unlabelled iron-loaded siderophore (0 to 10 μM). The mixtures were then centrifuged at 12,000 ***g*** for 3 min and the supernatants containing the unbound siderophore (labelled or not labelled) were removed. The tubes containing the cell pellet were counted for radioactivity in scintillation cocktail. The binding affinity constants (K_i) of the siderophores were calculated from the IC_{50} values, which were determined in competition experiments, according to the equation by Cheng & Prusoff:[55] $K_i = IC_{50}/(1 + L/K_d)$ where L is the concentration of radiolabelled ligand and K_d is its equilibrium dissociation constant determined experimentally. The K_d value of (Pch **1**/**2**)$_2$–Fe for FptA is 0.54($\pm$0.19) nM, as determined.[40]

Iron uptake

The iron uptake assays were carried out as reported for the FpvA/Pvd system.[56] *P. aeruginosa* PAO1, PAD07 and K2388 cells were prepared in 50 mM Tris–HCl (pH 8.0) at A_{600} of 1 and incubated at 37 °C. The transport assays were started by adding 10 nM (Pch **1**/**2**)$_2$–^{55}Fe, (neoPch **3**/**4**)2–^{55}Fe, Cep$_3$–^{55}Fe or the Pch analogues. Aliquots (100 μl) of the suspensions were removed at different times, filtered and the retained radioactivity was counted. The experiment was repeated once in the presence of 200 μM CCCP and once in the absence of cells.

Ligand docking

The starting conformations of the ligands **1**–**7** (Figure 1) were obtained by converting 2-D IsisDraw (Elsevier MDL, San Leandro, CA 94577, USA) sketches into 3-D coordinates using the Corina 3.10 program (Molecular Networks GmbH, D-91052 Erlangen, Germany). The automated docking of the manually ionised ligands to the FptA protein was done using seven speed-up settings of Gold2.2.[43] All organic molecules (water, LDAO, sulfate, ethylene glycol, ferric-Pch) were first removed from the protein structure and all hydrogen atoms automatically added using the Biopolymer module of the SYBYL package (Tripos, Inc., St. Louis, MO63144-2917, USA). The active site used for sampling the conformational space of the ligand was defined by a 12.5 Å radius sphere centred on the centre of mass of the ferric-Pch bound to the FptA protein. The calculation time was shortened by stopping the docking when the top three ranked solutions were within 1.5 Å rmsd. We can assume that these top solutions represent a reproducible conformation for the ligand. A maximum of ten conformations for each ligand were saved in standard mol2 format (Triptos, Inc., St. Louis, MO63144-2917, USA) and analysed using the Silver1.0 program (The Cambridge Crystallographic Data Centre, Cambridge, CB2 1EZ, UK).

Acknowledgements

This work was funded by the Centre National de la Recherche Scientifique (Programme Physique et Chimie du Vivant), the Ministère de l'Enseignement Supérieur, de la Recherche et de la Technologie (ACC-SDV5) and the association "Vaincre la Mucoviscidose." K.P. was supported by a grant from the Canadian Institutes of Health Research.

References

1. Høiby, N. & Fredericksen, B. (2000). Microbiology of cystic fibrosis. In Cystic Fibrosis (Hodson, M. E. & Geddes, D. M., eds), 2nd edit., pp. 83–107, Arnold, London.
2. Lyczak, J. B., Cannon, C. L. & Pier, G. B. (2000). Establishment of *Pseudomonas aeruginosa* infection: lessons from a versatile opportunist. *Microbes Infect.* **2**, 1051–1060.
3. Miller, P. J. & Wenzel, R. P. (1987). Etiologic organisms as independent predictors of death and morbidity associated with bloodstream infections. *J. Infect. Dis.* **156**, 471–477.
4. Boukhalfa, H. & Crumbliss, A. L. (2002). Chemical aspects of siderophore mediated iron transport. *Biometals*, **15**, 325–339.
5. Braun, V. (2001). Iron uptake mechanisms and their regulation in pathogenic bacteria. *Int. J. Med. Microbiol.* **291**, 67–79.
6. Abdallah, M. A. & Pattus, F. (2000). Siderophores and iron-transport in microorganisms. *J. Chin. Chem. Soc.* **47**, 1–20.
7. Rinehart, K. L., Jr, Staley, A. L., Wilson, S. R., Ankenbauer, R. G. & Cox, C. D. (1995). Stereochemical assignment of the pyochelins. *J. Org. Chem.* **60**, 2786–2791.
8. Cox, C. D. (1980). Iron uptake with ferripyochelin and ferriccitrate by *Pseudomonas aeruginosa*. *J. Bacteriol.* **142**, 581–587.
9. Sokol, P. A. (1984). Production of the ferripyochelin outer membrane receptor by *Pseudomonas* species. *FEMS Microbiol. Letters*, **23**, 313–317.
10. Cuppels, D. A., Stipanovic, R. D., Stoessl, A. & Stothers, J. B. (1987). The constitution and properties of a pyochelin-zinc complex. *Can. J. Chem.* **65**, 2126–2130.
11. Ankenbauer, R. G. & Quan, H. N. (1994). FptA, the Fe(III)-pyochelin receptor of *Pseudomonas aeruginosa*: a phenolate siderophore receptor homologous to hydroxamate siderophore receptors. *J. Bacteriol.* **176**, 307–319.
12. Cox, C. D. (1982). Effect of pyochelin on the virulence of *Pseudomonas aeruginosa*. *Infect. Immun.* **36**, 17–23.

13. Ankenbauer, R., Sriyosachati, S. & Cox, C. D. (1985). Effects of siderophores on the growth of *Pseudomonas aeruginosa* in human serum and transferrin. *Infect. Immun.* **49**, 132–140.
14. Cao, Z., Warfel, P., Newton, S. M. & Klebba, P. E. (2003). Spectroscopic observations of ferric enterobactin transport. *J. Biol. Chem.* **278**, 1022–1028.
15. DeWitte, J. J., Cox, A. D., Rasmussen, G. T. & Britigan, B. E. (2001). Assessment of structural features of the *Pseudomonas siderophore* pyochelin required for its ability to promote oxidant-mediated endothelial cell injury. *Arch. Biochem. Biophys.* **393**, 236–244.
16. Britigan, B. E., Rasmussen, G. T. & Cox, C. D. (1997). Augmentation of oxidant injury to human pulmonary epithelial cells by the *Pseudomonas aeruginosa* siderophore pyochelin. *Infect. Immun.* **65**, 1071–1076.
17. Takase, H., Nitanai, H., Hoshino, K. & Otani, T. (2000). Impact of siderophore production on *Pseudomonas aeruginosa* infections in immunosuppressed mice. *Infect. Immun.* **68**, 1834–1839.
18. Cox, C. D., Rinehart, K. L., Jr, Moore, M. L. & Cook, J. C., Jr (1981). Pyochelin: novel structure of an iron-chelating growth promoter for *Pseudomonas aeruginosa*. *Proc. Natl Acad. Sci. USA*, **78**, 4256–4260.
19. Ankenbauer, R. G., Toyokuni, T., Staley, A., Rinehart, K. L., Jr & Cox, C. D. (1988). Synthesis and biological activity of pyochelin, a siderophore of *Pseudomonas aeruginosa*. *J. Bacteriol.* **170**, 5344–5351.
20. Zamri, A. & Abdallah, M. A. (2000). An improved stereocontrolled synthesis of pyochelin, siderophore of *Pseudomonas aeruginosa* and *Burkholderia cepacia*. *Tetrahedron*, **56**, 249–256 corrigendum: Zamri, A., Abdallah, M. A. (2000). *Tetrahedron*, **56**, 93–97.
21. Ino, A. & Murabayashi, A. (2001). Total synthesis and absolute configuration of the siderophore yeriniabactin. *Tetrahedron*, **57**, 1897–1902.
22. Patel, H. M. & Walsh, C. T. (2001). *In vitro* reconstitution of the *Pseudomonas aeruginosa* nonribosomal peptide synthesis of pyochelin: characterization of backbone tailoring thiazoline reductase and *N*-methyltransferase activities. *Biochemistry*, **40**, 9023–9031.
23. Crosa, J. H. & Walsh, C. T. (2002). Genetics and assembly line enzymology of siderophore biosynthesis in bacteria. *Microbiol. Mol. Biol. Rev.* **66**, 223–249.
24. Serino, L., Reimmann, C., Visca, P., Beyeler, M., Chiesa, V. D. & Haas, D. (1997). Biosynthesis of pyochelin and dihydroaeruginoic acid requires the iron-regulated *pchDCBA* operon in *Pseudomonas aeruginosa*. *J. Bacteriol*, **179**, 248–257.
25. Reimmann, C., Serino, L., Beyeler, M. & Haas, D. (1998). Dihydroaeruginoic acid synthetase and pyochelin synthetase, products of the *pchEF* genes, are induced by extracellular pyochelin in *Pseudomonas aeruginosa*. *Microbiology*, **144**, 3135–3148.
26. Reimmann, C., Patel, H. M., Serino, L., Barone, M., Walsh, C. T. & Haas, D. (2001). Essential PchG-dependent reduction in pyochelin biosynthesis of *Pseudomonas aeruginosa*. *J. Bacteriol.* **183**, 813–820.
27. Barton, H. A., Johnson, Z., Cox, C. D., Vasil, A. I. & Vasil, M. L. (1996). Ferric uptake regulator mutants of *Pseudomonas aeruginosa* with distinct alterations in the iron-dependent repression of exotoxin A and siderophores in aerobic and microaerobic environments. *Mol. Microbiol.* **21**, 1001–1017.
28. Tseng, C. F., Burger, A., Mislin, G. L. A., Schalk, I. J., Yu, S. S. F., Chan, S. I. & Abdallah, M. A. (2006). Bacterial siderophores: the solution stoichiometry and coordination of the Fe(III) complexes of pyochelin and related compounds. *J. Biol. Inorg. Chem.* In the press.
29. Visca, P., Colotti, G., Serino, L., Verzili, D., Orsi, N. & Chiancone, E. (1992). Metal regulation of siderophore synthesis in *Pseudomonas aeruginosa* and functional effects of siderophore–metal complexes. *Appl. Environ. Microbiol.* **58**, 2886–2893.
30. Cobessi, D., Celia, H. & Pattus, F. (2005). Structure of ferric-pyochelin and its membrane receptor FptA from *Pseudomonas aeruginosa*. *J. Mol. Biol.* **352**, 893–904.
31. Ferguson, A. D., Braun, V., Fiedler, H. P., Coulton, J. W., Diederichs, K. & Welte, W. (2000). Crystal structure of the antibiotic albomycin in complex with the outer membrane transporter FhuA. *Protein Sci.* **9**, 956–963.
32. Ferguson, A. D., Chakraborty, R., Smith, B. S., Esser, L., van der Helm, D. & Deisenhofer, J. (2002). Structural basis of gating by the outer membrane transporter FecA. *Science*, **295**, 1715–1719.
33. Buchanan, S. K., Smith, B. S., Venkatramani, L., Xia, D., Esser, L., Palnitkar, M. *et al*. (1999). Crystal structure of the outer membrane active transporter FepA from *Escherichia coli*. *Nature Struct. Biol.* **6**, 56–63.
34. Locher, K. P., Rees, B., Koebnik, R., Mitschler, A., Moulinier, L., Rosenbusch, J. P. & Moras, D. (1998). Transmembrane signaling across the ligand-gated FhuA receptor: crystal structures of free and ferrichrome-bound states reveal allosteric changes. *Cell*, **95**, 771–778.
35. Yue, W. W., Grizot, S. & Buchanan, S. K. (2003). Structural evidence for iron-free citrate and ferric citrate binding to the TonB-dependent outer membrane transporter FecA. *J. Mol. Biol.* **332**, 353–368.
36. Ferguson, A. D., Hofmann, E., Coulton, J. W., Diederichs, K. & Welte, W. (1998). Siderophore-mediated iron transport: crystal structure of FhuA with bound lipopolysaccharide. *Science*, **282**, 2215–2220.
37. Klumpp, C., Burger, A., Mislin, G. L. & Abdallah, M. A. (2005). From a total synthesis of cepabactin and its 3:1 ferric complex to the isolation of a 1:1:1 mixed complex between iron (III), cepabactin and pyochelin. *Bioorg. Med. Chem. Letters*, **15**, 1721–1754.
38. Lin, Y., Helquist, P. & Miller, M. (1999). Synthesis and biological evaluation of a siderophore–virginiamycin conjugate. *Synthesis*, 1510–1514.
39. Hennard, C., Truong, Q. C., Desnottes, J. F., Paris, J. M., Moreau, N. J. & Abdallah, M. A. (2001). Synthesis and activities of pyoverdin–quinolone adducts: a prospective approach to a specific therapy against *Pseudomonas aeruginosa*. *J. Med. Chem.* **44**, 2139–2151.
40. Budzikiewicz, H. (2001). Siderophore–antibiotic conjugates used as trojan horses against *Pseudomonas aeruginosa*. *Curr. Top. Med. Chem.* **1**, 73–82.
41. Hoegy, F., Celia, H., Mislin, G. L., Vincent, M., Gallay, J. & Schalk, I. J. (2005). Binding of iron-free siderophore, a common feature for siderophore outer membrane receptors of *Escherichia coli* and *Pseudomonas aeruginosa*. *J. Biol. Chem.* **280**, 20222–20230.
42. Stintzi, A., Barnes, C., Xu, J. & Raymond, K. N. (2000). Microbial iron transport *via* a siderophore shuttle: a membrane ion transport paradigm. *Proc. Natl Acad. Sci. USA*, **97**, 10691–10696.
43. Verdonk, M. L., Cole, J. C., Hartshorn, M. J., Murray, C. W. & Taylor, R. D. (2003). Improved protein–ligand docking using GOLD. *Proteins: Struct. Funct. Genet.* **52**, 609–623.

44. Darling, P., Chan, M., Cox, A. D. & Sokol, P. A. (1998). Siderophore production by cystic fibrosis isolates of *Burkholderia cepacia*. *Infect. Immun.* **66**, 874–877.
45. Stover, C. K., Pham, X. Q., Erwin, A. L., Mizoguchi, S. D., Warrener, P., Hickey, M. J. *et al*. (2000). Complete genome sequence of *Pseudomonas aeruginosa* PA01, an opportunistic pathogen. *Nature*, **406**, 959–964.
46. Schalk, I. J., Kyslik, P., Prome, D., van Dorsselaer, A., Poole, K., Abdallah, M. A. & Pattus, F. (1999). Copurification of the FpvA ferric pyoverdin receptor of *Pseudomonas aeruginosa* with its iron-free ligand: implications for siderophore-mediated iron transport. *Biochemistry*, **38**, 9357–9365.
47. Schalk, I. J., Hennard, C., Dugave, C., Poole, K., Abdallah, M. A. & Pattus, F. (2001). Iron-free pyoverdin binds to its outer membrane receptor FpvA in *Pseudomonas aeruginosa*: a new mechanism for membrane iron transport. *Mol. Microbiol.* **39**, 351–360.
48. Clément, E., Mesini, P. J., Pattus, F., Abdallah, M. A. & Schalk, I. J. (2004). The binding mechanism of pyoverdin with the outer membrane receptor FpvA in *Pseudomonas aeruginosa* is dependent on its iron-loaded status. *Biochemistry*, **43**, 7954–7965.
49. Schalk, I. J., Yue, W. W. & Buchanan, S. K. (2004). Recognition of iron-free siderophores by TonB-dependent iron transports. *Mol. Microbiol.* **54**, 14–22.
50. Schlegel, K., Taraz, K. & Budzikiewicz, H. (2004). The stereoisomers of pyochelin, a siderophore of *Pseudomonas aeruginosa*. *Biometals*, **17**, 409–414.
51. Mislin, G., Burger, A. & Abdallah, M. (2004). Synthesis of new thiazole analogs of pyochelin, a siderophore of *Pseudomonas aeruginosa* and *Burkholderia cepacia*. A new conversion of thiazolines into thiazoles. *Tetrahedron*, **60**, 12139–12145.
52. Royle, P. L., Matsumoto, H. & Holloway, B. W. (1981). Genetic circularity of the *Pseudomonas aeruginosa* PAO chromosome. *J. Bacteriol.* **145**, 145–155.
53. Heinrichs, D. E. & Poole, K. (1996). PchR, a regulator of ferripyochelin receptor gene (*fptA*) expression in *Pseudomonas aeruginosa*, functions both as an activator and as a repressor. *J. Bacteriol.* **178**, 2586–2592.
54. Demange, P., Wendenbaum, S., Linget, C., Mertz, C., Cung, M. T., Dell, A. & Abdallah, M. A. (1990). Bacterial siderophores: structure and NMR assigment of pyoverdins PaA, siderophores of *Pseudomonas aeruginosa* ATCC 15692. *Biol. Metals*, **3**, 155–170.
55. Cheng, Y. C. & Prusoff, W. H. (1973). Relationship between the inhibition constant (K_1) and the concentration of inhibitor which causes 50 per cent inhibition (I50) of an enzymatic reaction. *Biochem. Pharmacol.* **22**, 3099–3108.
56. Schalk, I. J., Abdallah, M. A. & Pattus, F. (2002). Recycling of pyoverdin on the FpvA receptor after ferric pyoverdin uptake and dissociation in *Pseudomonas aeruginosa*. *Biochemistry*, **41**, 1663–1671.
57. Cobessi, D., Celia, H. & Pattus, F. (2004). Crystallization and X-ray diffraction analyses of the outer membrane pyochelin receptor FptA from *Pseudomonas aeruginosa*. *Acta Crystallog. sect. D*, **60**, 1919–1921.
58. Exner, T. E., Keil, M., Moeckel, G. & Brickmann, J. (1998). Identification of substrate channels and protein cavities. *J. Mol. Model.* **4**, 340–343.

Edited by I. B. Holland

(Received 14 November 2005; received in revised form 19 January 2006; accepted 23 January 2006)
Available online 8 February 2006